

# UCLA

## UCLA Previously Published Works

### Title

Multi-vendor reliability of arterial spin labeling perfusion MRI using a near-identical sequence: Implications for multi-center studies

### Permalink

<https://escholarship.org/uc/item/26g819kj>

### Authors

Mutsaerts, Henri JMM  
van Osch, Matthias JP  
Zelaya, Fernando O  
[et al.](#)

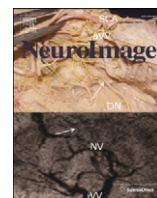
### Publication Date

2015-06-01

### DOI

10.1016/j.neuroimage.2015.03.043

Peer reviewed



## Multi-vendor reliability of arterial spin labeling perfusion MRI using a near-identical sequence: Implications for multi-center studies



Henri J.M.M. Mutsaerts<sup>a,\*</sup>, Matthias J.P. van Osch<sup>b</sup>, Fernando O. Zelaya<sup>c</sup>, Danny J.J. Wang<sup>d</sup>, Wibeke Nordhøy<sup>e</sup>, Yi Wang<sup>d</sup>, Stephen Wastling<sup>c</sup>, Maria A. Fernandez-Seara<sup>f</sup>, E.T. Petersen<sup>g</sup>, Francesca B. Pizzini<sup>h</sup>, Sameeha Fallatah<sup>i</sup>, Jeroen Hendrikse<sup>g</sup>, Oliver Geier<sup>e</sup>, Matthias Günther<sup>j,k</sup>, Xavier Golay<sup>i</sup>, Aart J. Nederveen<sup>a</sup>, Atle Bjørnerud<sup>e,l</sup>, Inge R. Grooten<sup>m</sup>

<sup>a</sup> Department of Radiology, Academic Medical Center, Amsterdam, The Netherlands

<sup>b</sup> C.J. Gorter Center for High Field MRI, Department of Radiology, Leiden University Medical Center, Leiden, The Netherlands

<sup>c</sup> Department of Neuroimaging, Institute of Psychiatry, Psychology and Neuroscience, Kings College London, London, UK

<sup>d</sup> Department of Neurology, UCLA, Los Angeles, USA

<sup>e</sup> The Intervention Center, Oslo University Hospital, Oslo, Norway

<sup>f</sup> Division of Neuroscience, Center for Applied Medical Research (CIMA), University of Navarra, Pamplona, Spain

<sup>g</sup> Department of Radiology, University Medical Center, Utrecht, The Netherlands

<sup>h</sup> Division of Neuroradiology, University of Verona, Verona, Italy

<sup>i</sup> Brain Repair & Rehabilitation, Institute of Neurology, UCL, London, UK

<sup>j</sup> Fraunhofer MEVIS, Bremen, Germany

<sup>k</sup> MR Physics, University of Bremen, Bremen, Germany

<sup>l</sup> Department of Physics, University of Oslo, Oslo, Norway

<sup>m</sup> Department of Psychology, Institute of Social Sciences, University of Oslo, Oslo, Norway

### ARTICLE INFO

#### Article history:

Received 8 December 2014

Accepted 16 March 2015

Available online 24 March 2015

#### Keywords:

Arterial spin labeling

Cerebral blood flow

Inter-vendor

Repeatability

Reproducibility

### ABSTRACT

**Introduction:** A main obstacle that impedes standardized clinical and research applications of arterial spin labeling (ASL), is the substantial differences between the commercial implementations of ASL from major MRI vendors. In this study, we compare a single identical 2D gradient-echo EPI pseudo-continuous ASL (PCASL) sequence implemented on 3T scanners from three vendors (General Electric Healthcare, Philips Healthcare and Siemens Healthcare) within the same center and with the same subjects.

**Material and methods:** Fourteen healthy volunteers (50% male, age  $26.4 \pm 4.7$  years) were scanned twice on each scanner in an interleaved manner within 3 h. Because of differences in gradient and coil specifications, two separate studies were performed with slightly different sequence parameters, with one scanner used across both studies for comparison. Reproducibility was evaluated by means of quantitative cerebral blood flow (CBF) agreement and inter-session variation, both on a region-of-interest (ROI) and voxel level. In addition, a qualitative similarity comparison of the CBF maps was performed by three experienced neuro-radiologists.

**Results:** There were no CBF differences between vendors in study 1 ( $p > 0.1$ ), but there were CBF differences of 2–19% between vendors in study 2 ( $p < 0.001$  in most gray matter ROIs) and 10–22% difference in CBF values obtained with the same vendor between studies ( $p < 0.001$  in most gray matter ROIs). The inter-vendor inter-session variation was not significantly larger than the intra-vendor variation in all ( $p > 0.1$ ) but one of the ROIs ( $p < 0.001$ ).

**Conclusion:** This study demonstrates the possibility to acquire comparable cerebral CBF maps on scanners of different vendors. Small differences in sequence parameters can have a larger effect on the reproducibility of ASL than hardware or software differences between vendors. These results suggest that researchers should strive to employ identical labeling and readout strategies in multi-center ASL studies.

© 2015 Elsevier Inc. All rights reserved.

**Abbreviations:** ASL, arterial spin labeling; CBF, cerebral blood flow; DARTEL, diffeomorphic anatomical registration analysis using exponentiated lie algebra; EPI, echo-planar imaging; GM, gray matter; MRI, magnetic resonance imaging; PLD, post-label delay; PCASL, pseudo-continuous ASL; ROI, region of interest; SDΔCBF, standard deviation of the paired inter-session CBF difference; SNR, signal-to-noise ratio; WM, white matter; wsCV, within-subject coefficient of variation.

\* Corresponding author at: Department of Radiology, G1-230, Academic Medical Center, Meibergdreef 9, 1105 AZ Amsterdam, The Netherlands. Fax: +31 20 56 69119.

E-mail address: [henkjanmutsaerts@gmail.com](mailto:henkjanmutsaerts@gmail.com) (H.J.M.M. Mutsaerts).

## Introduction

Through a number of methodological advances, arterial spin labeling (ASL) perfusion MRI has reached a level that allows its application in multiple clinical and research applications for the visualization and quantification of cerebral blood flow (CBF) (Dette et al., 2012; Williams et al., 1992). Since ASL is non-invasive and offers absolute CBF quantification, it is an attractive tool compared to alternative perfusion modalities (Golay et al., 2004; Hendrikse et al., 2012). Furthermore, quantitative ASL CBF maps are reproducible and comparable with perfusion measurements from the “gold standard”  $H_2O^{15}$ -PET (Heijtel et al., 2014; Petersen et al., 2010; Xu et al., 2010). Implementations of ASL are commercially available on all major MRI systems and the number of clinical applications is continuously growing. Measurements of regional CBF promise clinical value in a variety of common neurological disorders, such as cerebrovascular disease, epilepsy, neurodegeneration and brain tumors, and ASL is recognized as a particularly valuable research tool for cognitive and pharmacological neuroscience (Deibler et al., 2008; Wang et al., 2011).

One obstacle that impedes standardized clinical and research applications of ASL, is the substantial differences in the commercial implementations of ASL from the major MRI vendors (Alsop et al., 2015). A variety of possible labeling and readout strategies exists, and each vendor has implemented a different combination of labeling and readout strategies for their commercial ASL release (Alsop et al., 2015). General Electric (GE) Healthcare offers pseudo-continuous ASL (PCASL) with a segmented 3D spiral fast spin-echo (FSE) readout, Philips Healthcare has PCASL paired with a single-shot 2D echo-planar imaging (EPI) readout and Siemens Healthcare provides pulsed ASL (PASL) combined with a segmented 3D gradient and spin-echo (GRASE) readout (Aslan et al., 2010; Gunther et al., 2005; Ye et al., 2000).

These labeling and readout differences between product sequences produce qualitatively different perfusion-weighted images, which can be visually appreciated on a single-subject level as shown in Fig. 1a (Chen et al., 2011; Kilroy et al., 2014). On a group level, it is currently not possible to compare CBF-values from a single region of interest (ROI) in a multi-center study, mainly because of differences in readout between sequences from different vendors (Mutsaerts et al., 2014; Vidorreta et al., 2012). Global CBF-values, however, show quantitative agreement between vendors (Mutsaerts et al., 2014). Furthermore, the inter-vendor global CBF inter-session variation is comparable to the intra-vendor global CBF variation (Chen et al., 2011; Mutsaerts et al., 2014). These observations support the possibility of future multi-center ASL research, if all vendors could implement an identical ASL sequence.

The current study aims to assess multi-vendor ASL CBF variations using a near-identical sequence across vendors, with the same labeling

and readout approach. PCASL was selected as a labeling strategy, because of its wide compatibility with all platforms and superior labeling efficiency for single time-point CBF measurements (Alsop et al., 2015; Chen et al., 2011; Dai et al., 2008). A multi-slice single-shot 2D EPI readout was selected because of its availability on all systems and as it has been used in the majority of previous ASL studies (Alsop et al., 2015). Because of differences in gradient and RF coil specifications between two vendor systems available for our study, two 2D echo-planar imaging (EPI) PCASL sequences were used with slightly different labeling and readout parameters. These will be referred to as study 1 and 2. For one vendor system, both variants of our sequence could be implemented, enabling an additional intra-vendor comparison of these slightly different sequences.

## Materials and methods

### MRI scanners

Three 3 T MRI scanners were used in this single-center multi-vendor comparison: GE Signa HDxt (2006, 60 cm bore opening, General Electric Healthcare, Milwaukee, WI, US), Philips Achieva (2007, 60 cm bore opening, Philips Healthcare, Best, The Netherlands) and Siemens Skyra (2011, 70 cm bore opening, Siemens Healthcare, Erlangen, Germany). None of the vendors were involved in designing or conducting this study, none had access to the data, and none were involved in data analysis or preparation of this manuscript. Because the main purpose of the study was to compare the inter- and intra-vendor reproducibility, without addressing the performance of each vendor system explicitly, vendor and coil names were anonymized by pseudo-randomly reordering the vendor names into vendor A, B and C. Vendor A was included in both studies because its gradient and RF coil specifications allowed sequence implementation identical to both vendor B and C. The scanners of vendor A and B were equipped with 8-channel head coils, whereas the scanner of vendor C was equipped with a 20-channel head-neck coil. Vendor A and C were separated by a five-minute walk, whereas vendor B was located at 20 minutes traveling distance by public transport from the location of the two other scanners.

### Study design

Both the local regional ethics committee and the local University Hospital internal ethical review board approved the study and all subjects provided written informed consent. In addition to standard MRI exclusion criteria, subjects with history of brain or psychiatric disease or use of medication — except for oral contraceptives — were excluded. To minimize physiological perfusion fluctuation, physical exercise and consumption of alcohol or recreational drugs was prohibited for 24 h prior to scanning, except for caffeine or nicotine, which were restricted

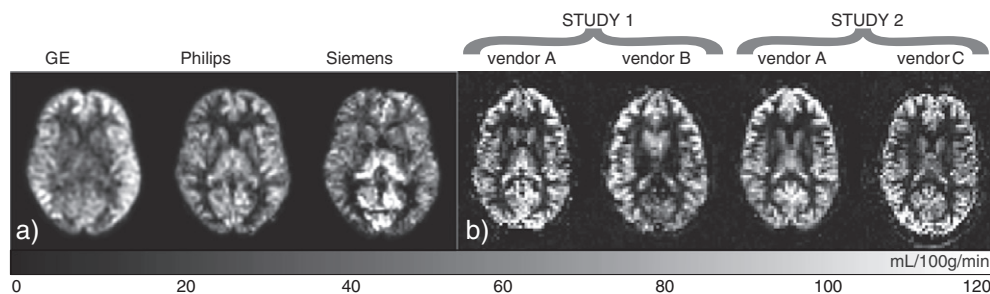


**Fig. 1.** a) Perfusion-weighted maps from a single subject scanned with product sequences from GE (PCASL with a 3D spiral FSE readout), Philips (PCASL with a 2D EPI readout) and Siemens (PASL with a 3D GRASE readout). Sequence parameters included PLD = 1525 ms, 4 time points, true axial (GE), PLD = 1525 ms (Philips) and TI = 2300 ms, T11 = 80 ms, 4 time points (Siemens). Because of differences in voxel size, these maps were linearly registered, re-sliced and skull-stripped. b) Raw perfusion-weighted maps from a single representative subject scanned with the sequence used in the current study (parameters shown in Tables 1 and 2). All perfusion weighted maps were scaled to have a mean gray matter cerebral blood flow of 60 mL/100 g/min.

for 6 h before the scanning sessions (Golay, 2009). In both studies, each participant was scanned twice on two different scanners (i.e. four MRI examinations per participant per study) within 3 h, to limit the effect of physiological perfusion fluctuations (Fig. 2). Order effects were avoided by randomly starting with either vendor A or B (study 1) or with either vendor A or C (study 2). Foam padding inside the head coil was used to restrict head motion during scanning. Subjects were awake and had their eyes closed during all ASL scans. In all sessions, PCASL acquisitions were performed 10 min after the positioning of the subject in the scanner to allow perfusion to stabilize.

### Acquisition

Each scan session included a balanced PCASL sequence with a single-shot gradient-echo EPI readout and a 1 mm isotropic 3D T1-weighted structural scan for segmentation and registration purposes. Detailed similarities and differences between the PCASL protocols are summarized in Tables 1 and 2. The field-of-view was positioned parallel to the anterior–posterior commissure (ACPC) line. Due to restrictions imposed by two of the MR systems the labeling plane was fixed parallel to the stack of imaging slices.

### Post-processing: quantification

Matlab 7.12.0 (MathWorks, MA, USA) and Statistical Parametric Mapping 8 (SPM8, Wellcome Trust Center for Neuroimaging, University College London, UK) were used for post-processing and statistical analyses. Motion parameters were estimated to test whether the net displacement vector – the root mean square of three translations and three rotations – differed between sessions, vendors or studies (Wilcoxon Rank-Sum test). To avoid confounding effects from motion correction due to possible signal-to-noise ratio (SNR) differences between vendors or coils, no motion correction was applied. The first five control and label pairs were discarded to avoid any non-steady state effects in the MRI signal. The remaining control ( $M_{\text{control}}$ ) and label ( $M_{\text{label}}$ ) images were pair-wise subtracted and averaged. The average control image was used to derive  $M_0$ , by assuming a fixed single T1 of tissue (equal to  $T_{1\text{GM}}$  described below). These perfusion-weighted images were quantified into CBF maps using a single compartment model (Alsop et al., 2015):

$$\text{CBF [mL/100g/min]} = \frac{6000\lambda(M_{\text{control}} - M_{\text{label}}) e^{PLD/T_{1a}} (1 - e^{-\frac{TR}{T_{1\text{GM}}}})}{2\alpha T_{1a} M_{\text{control}} (1 - e^{-\frac{\tau}{T_{1a}}})} \quad (1)$$

where  $\lambda$  is the brain–blood partition coefficient (0.9 mL/g), PLD is the post-label delay of each slice (Table 2);  $T_{1a}$  is the longitudinal relaxation time of arterial blood (1650 ms),  $\alpha$  is the labeling efficiency (85%) and  $\tau$  is the label duration (Table 2) (Aslan et al., 2010; Herscovitch and Raichle, 1985; Lu et al., 2004).  $1 - e^{(-TR/T_{1\text{GM}})}$  corrects for the incomplete signal recovery of the control images;  $TR$  is the repetition time (Table 2) and  $T_{1\text{GM}}$  is the longitudinal relaxation time of gray matter (GM)

**Table 1**  
Identical labeling and readout parameters.

Labeling approach	Balanced waveform PCASL
Labeling pulse shape	Hanning
Mean labeling gradient	0.6 mT/m
Max labeling gradient	6 mT/m
Labeling flip angle	25°
Labeling duration	1771 ms
Initial post-label delay	1800 ms
Labeling position	Fixed, 9 cm below ACPC
Readout approach	Single shot EPI
Slices	20
Slice thickness	6 mm
Matrix size	64 × 64
Field of view	224 × 224 mm
Fat suppression	SPIR
Parallel imaging	Off
B1-filtering	Off
Partial Fourier	Off
Background suppression	Off
Vascular suppression	Off
Label-control pairs	70

ACPC = anterior–posterior commissure; EPI = echo-planar imaging; PCASL = pseudo-continuous arterial spin labeling; SPIR = spectral presaturation by inversion recovery.

(1240 ms). The same quantification parameters were used for GM and white matter (WM).

### Post-processing: spatial normalization

A single 3D T1-weighted anatomical scan for each subject ( $n = 14$ ) was segmented into GM and WM tissue probability maps. To avoid registration effects from differences in the T1-weighted reference images, the T1-weighted images from a single vendor (vendor A) were used. All CBF maps were transformed into anatomical space by a rigid-body registration of the average control image to the skull-stripped T1-weighted scan. To spatially normalize both anatomical differences between subjects and residual EPI geometric distortion differences between vendors, a three-stage normalization strategy was applied, based on DARTEL (Diffeomorphic Anatomical Registration analysis using Exponentiated Lie algebra) (Ashburner, 2007). First, a T1-based DARTEL template was created using the GM and WM probability maps from the T1-weighted scans. The resulting DARTEL flow fields were applied to the average control images of all vendors, removing anatomical differences between subjects. Afterwards, the normalized mean EPI control images were segmented into GM and WM probability maps from which vendor-specific EPI-based DARTEL templates were created. The resulting flow fields were applied to the mean control images, removing residual geometric differences between subjects (Petr et al., 2014). Finally, the vendor-specific EPI-based DARTEL templates were warped to the T1-based DARTEL template, removing geometric distortion differences between vendors. All transformations were applied to the corresponding CBF maps.

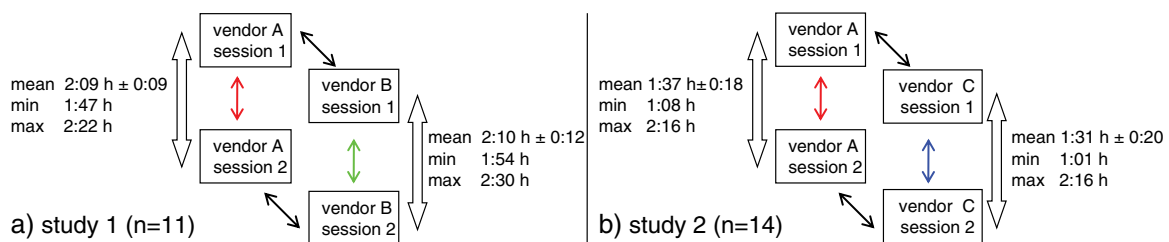


**Fig. 2.** Study design and inter-session time differences between vendors of both studies (large transparent arrows). The small filled arrows correspond to the comparisons performed in this study: intra-vendor vendor A (red), intra-vendor vendor B (green), intra-vendor vendor C (blue), inter-vendor comparison (black). Note that the comparison between studies for vendor A is not indicated by an arrow.

**Table 2**  
Different labeling and readout parameters.

	Study 1		Study 2	
	Vendor A	Vendor B	Vendor A	Vendor C
Inter-pulse time	1.24 ms	1.24 ms	1.15 ms	1.15 ms
Shimming labeling plane	Yes	No	Yes	Yes
TE	28 ms	28 ms	21 ms	21 ms
TR	4800 ms	4800 ms	4700 ms	4700 ms
Slice readout time	60.9 ms	61.5 ms	50.2 ms	52 ms
PLD range	1771–2928 ms	1771–2940 ms	1771–2725 ms	1771–2760 ms
Total scan duration	11:12 min	11:12 min	10:58 min	10:58 min

PLD = post-label delay; TE = echo time; TR = readout time.

### Data analysis

Reproducibility was evaluated by means of quantitative CBF agreement and inter-session variation, testing whether the mean CBF is equal for different vendors and whether the inter-vendor inter-session variation is equal to the intra-vendor variation. These hypotheses were tested quantitatively on both a region of interest (ROI) and on a voxel level. In addition, a qualitative similarity comparison of the major features of the CBF maps was performed by three neuro-radiologists.

All intra-vendor reproducibility analyses were based on a comparison of session 1 with session 2 within each vendor ( $n = 11$  and  $n = 14$  for study 1 (vendor A and B) and 2 (vendor A and C) respectively, colored arrows in Fig. 2). All inter-vendor reproducibility analyses were based on pooled comparisons of both the first sessions between vendors and the second sessions between vendors ( $n = 22$  and  $n = 28$  for study 1 and 2 respectively, black arrows in Fig. 2). To compare both studies, the results from vendor A will be used because of its participation in both studies (first 11 subjects only). All reproducibility analyses were based on the mean CBF of the compared sessions and on the standard deviation of the paired inter-session CBF difference ( $SD\Delta CBF$ ). The within-subject coefficient of variation (wsCV) – a normalized parameter of inter-session variation – was defined as the ratio of  $SD\Delta CBF$  to the mean CBF of both compared sessions (Bland and Altman, 1999):

$$wsCV = 100\% \frac{SD\Delta CBF}{\text{mean CBF}}. \quad (2)$$

### Data analysis: ROI definition

Subject-specific total cerebral GM and deep cerebral WM masks were obtained by thresholding GM and WM probability maps at 80% and 99% tissue probabilities respectively. WM masks were threefold eroded to avoid GM contamination (Mutsaerts et al., 2013). ROIs of anterior, middle and posterior flow territories (supplied by the anterior, middle and posterior cerebral artery respectively) were created from standard vascular territory templates (Tatu et al., 1998) and ROIs associated with age-related dementia (anterior and posterior cingulate, precuneus) were created from the Wake Forest University Pick-atlas (<http://fmri.wfubmc.edu/cms/software>). All standard ROIs were masked with the subject-specific GM masks. Since almost all distributions deviated from normal – according to the Shapiro–Wilk test – the median was used to summarize CBF within a ROI.

### Data analysis: voxel-based comparison

To assess reproducibility differences spatially, CBF- and wsCV-values were computed for each voxel. In order to visualize how much larger or smaller the inter-vendor  $SD\Delta CBF$  was than the intra-vendor  $SD\Delta CBF$ , a

voxel-wise variation ratio map was created according to the following equation (Asllani et al., 2008):

$$100\% \frac{SD\Delta CBF_{\text{inter-vendor}}}{SD\Delta CBF_{\text{intra-vendor}}}. \quad (3)$$

This map was created for each study, including the two inter- and the two intra-vendor inter-session comparisons (black and colored arrows respectively in Fig. 2). If the inter-vendor covariance is equal to the intra-vendor covariance, we expect a mean variation ratio of 100%. Individual GM CBF histograms (80 bins, range –10–110 mL/100 g/min) were averaged to generate a group-level histogram. GM wsCV (80 bins, range 0–100%) and ratio (80 bins, range 20–180%) histograms were generated.

Both on an ROI and on a voxel level, mean CBF differences between vendors were tested for significance using a paired two-tailed Student's t-test. The Levene's test was used to test whether the inter-vendor inter-session  $SD\Delta CBF$  was significantly different from the intra-vendor inter-session  $SD\Delta CBF$ .

### Data analysis: qualitative similarity index

In order to compare the inter- and intra-vendor reliability qualitatively, inter- and intra-vendor head-to-head CBF maps were rated for their similarity by three neuroradiologists (FBP, SF and JH) with at least five years of experience with ASL. The following comparisons were included: intra-vendor comparisons (colored arrows Fig. 2) for vendor A and B (study 1,  $n = 2 * 11$ ) and vendor A and C (study 2,  $n = 2 * 14$ ) as well as inter-vendor comparisons (black arrows Fig. 2) for vendor A vs. B sessions 1 and 2 ( $n = 2 * 11$ ) and vendor A vs. C sessions 1 and 2 ( $n = 2 * 14$ ), adding up to 100 comparisons in total. The 100 comparisons were pseudo-randomized and only the skull-stripped, spatially normalized cerebrum was included, to avoid any recognizable vendor-specific geometric distortion or susceptibility artifacts. The spatially normalized CBF maps were divided into 20 slices and rescaled slice-wise, such that the mean GM CBF of each slice was equal for the compared sessions. All comparisons were converted into color-scaled DICOM images containing the two compared sessions per image, horizontally side by side.

After giving a first general impression for the total GM, the raters provided an ordinal score from 1 to 5 for the anterior, middle and posterior flow territories and for the deep GM consecutively, based on similarity of morphology and intensity. Similarity scores were defined as 1) poor, 2) fair, 3) moderate, 4) good and 5) excellent. Krippendorff's alpha was used to quantify the inter-rater agreement. The mean rating of all three neuroradiologists was used for analysis. Intra- and inter-vendor similarity scale histograms (5 bins, range 1–5) were generated for the abovementioned ROIs. A two-sample t-test was used to test whether the inter-vendor similarity was lower than the intra-vendor similarity. Significance was thresholded at  $p = 0.05$  in all analyses.

## Results

### Subjects

Fourteen healthy volunteers (50% male, mean age  $26.4 \pm 4.7$  (SD) years) were included, of which 11 (5 men, mean age  $25.2 \pm 4.5$  years) were included in study 1 and all 14 subjects were included in study 2.

### Motion

The mean motion was not normally distributed for all vendors and sessions. Mean motion did not differ between vendors, sessions or studies ( $p > 0.1$  for all comparisons).

### Session timing

The intra-vendor inter-session time intervals did not differ between vendors in study 1 ( $p = 0.6$ , paired t-test) or study 2 ( $p = 0.3$ ), but were 31 min longer for vendor A study 1 than for vendor A study 2 ( $p < 0.01$ , Fig. 2). The ASL scans of study 1 ( $18 \text{ h}50 \pm 2 \text{ h}00$ ) were performed 2 h20 later on each day ( $p < 0.01$ ) than those of study 2 ( $16 \text{ h}30 \pm 3 \text{ h}20$ ). Study 1 was performed 2.7 weeks after study 2 ( $p < 0.01$ ).

### Region-based comparison

Both the ROI-based median CBF-values (Table 3) and paired inter-session differences (summarized by wsCV in Table 4) were normally distributed. For all ROIs the mean CBF did not differ significantly between vendor A and B in study 1 ( $p > 0.1$ ). The mean regional CBF of vendor A was 2–19% higher ( $p < 0.001$  in most GM ROIs) than the mean regional CBF of vendor C in study 2, with the largest differences in the posterior flow territory and in the posterior cingulate gyrus. In addition, CBF values of vendor A in study 1 (vendor A and B) were 10–22% lower ( $p < 0.001$  in most GM ROIs) than those of the same vendor in study 2 (vendor A and C). Except for the posterior cingulate cortex in study 1 ( $p < 0.001$ ), there were no differences between the intra- and inter-vendor  $\text{SD}\Delta\text{CBF}$  for study 1 ( $p > 0.1$ ) or for study 2 ( $p > 0.2$ ) (Table 4). However, the  $\text{SD}\Delta\text{CBF}$  of vendor A was 1.5–2 times as large for the sequence in study 1 as compared to the sequence in study 2, which was significant for the anterior ( $p = 0.04$ ) and posterior flow territory ( $p = 0.04$ ) and precuneus ( $p = 0.03$ ).

### Voxel-based comparison

The CBF maps of a single representative subject show that visually the cortical and subcortical GM–WM differentiation was more

comparable between vendors with the near-identical sequences (Fig. 1b) than with product sequences (Fig. 1a). The group mean CBF maps and CBF histograms (Fig. 3) of vendor A and B (study 1) appeared very similar visually. There was only a slight difference in the inferior part of the cerebellum and in the orbito-frontal lobe and a small second peak in the lower range of the histogram of vendor B. However, the mean CBF maps of vendor A and C (study 2) showed significant intensity differences, most notably in the posterior flow territory and in the cerebellum. The histograms of vendors A and C have an identical appearance, except for a shift of the peak location for vendor A to higher CBF as compared to vendor C. Interestingly, the largest difference was observed when the results of the same vendor (A) were compared between the sequences of study 1 and 2 (Fig. 5a). The mean CBF and CBF distributions on histograms were lower and wider in study 1 compared to study 2 and for most voxels on the parametric maps the CBF-values were larger for study 2 than for study 1.

In both studies, the wsCV maps and histograms (Fig. 4) appeared similar between vendors, with only slightly larger variation for vendor A compared to vendor B (study 1) throughout the brain and for vendor C compared to vendor A (study 2) in the posterior flow territory. Areas of largest variation were the deep GM, posterior flow territory (including the cerebellum) and the orbito-frontal cortex. The inter-vendor wsCV maps showed the same spatial distribution as the intra-vendor maps, but the overall wsCV was somewhat higher. Likewise, the inter- and intra-vendor wsCV histograms appeared similar, but the inter-vendor wsCV distribution was shifted towards higher values. Interestingly, the wsCV histograms of vendor A in study 1 were higher and wider than the histograms of the same vendor in study 2. The values on the wsCV maps of vendor A study 2 visually appeared lower and more homogeneous compared to vendor A study 1, which was shown to be significant in the majority of the voxels (Fig. 5b).

The inter- to intra-vendor variation ratio (Fig. 6) was heterogeneously distributed and ranged from 75–125% in the majority of voxels. Based on the histograms, the mean ratio was slightly higher than 100% and the distribution was approximately Gaussian, with slightly more voxels having a higher inter- than intra-vendor  $\text{SD}\Delta\text{CBF}$ . There were a few voxels with significantly higher inter- than intra-vendor  $\text{SD}\Delta\text{CBF}$ , which were mainly situated in the posterior flow territory for vendor A vs. B and spread throughout the brain for vendor A vs. C.

### Similarity scale

The inter-rater agreement of the visual similarity scale was moderate (Krippendorff's  $\alpha = 0.44$ – $0.57$ ) in most ROIs, but only fair in the deep GM ( $\alpha = 0.28$ ). There was no substantial inter-rater agreement

**Table 3**  
Cerebral blood flow.

	Study 1			Study 2			Study 1 vs. 2 %Δ Vendor A
	Vendor A	Vendor B	%Δ	Vendor A	Vendor C	%Δ	
<i>Whole brain regions</i>							
Total gray matter	48.9 (9.8)	49.6 (14.4)	1.4	57.1 (7.6)	53.8 (6.7)	†6.0	15.5†
Total white matter	14.3 (3.1)	13.0 (3.7)	10.1	15.9 (3.3)	15.1 (2.9)	4.8	10.2
GM–WM ratio	3.5 (0.7)	3.9 (1.0)	11.8	3.7 (0.6)	3.7 (0.8)	0.9	5.7
<i>Flow territories</i>							
Anterior	50.3 (10.2)	50.2 (14.9)	0.2	58.6 (8.2)	54.8 (7.5)	†6.6	15.2†
Middle	49.8 (9.6)	51.5 (14.3)	3.5	58.0 (7.8)	55.9 (6.5)	3.7	15.4†
Posterior	44.5 (12.2)	42.7 (15.6)	4.2	52.8 (8.2)	44.7 (8.4)	†16.7	17.0†
<i>Dementia regions</i>							
Anterior cingulate cortex	48.9 (12.7)	52.0 (15.4)	6.3	57.5 (8.3)	56.6 (7.7)	1.6	16.2*
Posterior cingulate cortex	46.8 (14.7)	44.4 (19.3)	5.3	58.4 (11.5)	48.0 (12.4)	†19.4	22.0†
Precuneus	51.6 (12.6)	49.0 (17.0)	5.2	59.7 (9.6)	52.1 (9.3)	†13.7	14.6*

Cerebral blood flow (CBF) (SD), shown in mL/100 g/min. %Δ represents the percentual difference between vendors within study 1 or 2 and between studies for the same vendor (vendor A) in the last column. CI = confidence interval. \* $p < 0.05$ , † $p < 0.001$ .

**Table 4**  
Inter-session within-subject coefficient of variation.

	Study 1				Study 2				Study 1 vs. 2
	Vendor A	Vendor B	Inter-vendor	Ratio	Vendor A	Vendor C	Inter-vendor	Ratio	Ratio vendor A
Total gray matter	15.9 (7.6)	15.4 (10.4)	20.5 (6.4)	1.3	9.1 (4.9)	8.2 (4.3)	11.3 (3.4)	1.3	1.8
<i>Flow territories</i>									
Anterior	18.4 (8.3)	14.6 (10.6)	21.9 (6.7)	1.3	10.2 (5.4)	9.9 (4.9)	11.6 (3.6)	1.2	1.8*
Middle	13.8 (7.3)	15.3 (10.4)	18.5 (6.2)	1.3	8.1 (4.9)	8.1 (4.2)	11.2 (3.3)	1.4	1.7
Posterior	23.4 (9.7)	22.3 (11.5)	32.4 (7.7)	1.4	13.1 (5.5)	16.6 (5.8)	17.3 (4.3)	1.2	1.8*
<i>Dementia regions</i>									
Anterior cingulate cortex	24.1 (10.4)	11.4 (10.7)	25.5 (7.5)	1.4	12.1 (5.6)	10.3 (5.1)	11.9 (3.6)	1.1	2.0
Posterior cingulate cortex	32 (12.4)	19.7 (13.7)	46.1 (10.2)	†1.8	21.2 (8.5)	30.8 (9.5)	22 (6.0)	0.8	1.5
Precuneus	23.9 (10.5)	17.7 (12.2)	29.4 (8.2)	1.4	12.4 (6.4)	17.9 (6.7)	14.4 (4.6)	1.0	1.9*

Within-subject coefficient of variation (wsCV) (confidence intervals), shown in percentages (%). Ratio represents the inter-/intra-vendor  $SD\Delta CBF$ -ratio. The study 1/study 2  $SD\Delta CBF$ -ratio for vendor A is shown in the last column. CI = confidence interval. \* $p < 0.05$ , † $p < 0.001$ .

difference between the intra-vendor (Krippendorff's  $\alpha = 0.27$ – $0.48$ ) and inter-vendor ( $\alpha = 0.26$ – $0.62$ ) comparisons.

For both the intra- and inter-vendor similarity, the average rate ranged from fair to good, and was 'moderate' in most ROIs (Fig. 7). In study 1, the inter-vendor similarity ( $2.7 \pm 0.2$ ) was on average  $10.8 \pm 2.3\%$  lower than the intra-vendor similarity ( $3.0 \pm 0.2$ ). In study 2, the inter-vendor similarity ( $3.4 \pm 0.3$ ) was on average  $8.8 \pm 4.8\%$  lower than the intra-vendor similarity ( $3.8 \pm 0.2$ ), which was significant for the total GM, posterior flow territory and deep GM. Whereas the similarity scale histograms of the total GM, anterior and middle

territories had similar means, the deep GM histogram was somewhat lower and the posterior flow territory histograms had the lowest mean. All histograms of study 2 had a smaller distribution and higher mean than the histograms of study 1 ( $p < 0.01$ ).

## Discussion

Using near-identical PCASL sequences, we were able to acquire similar CBF images on 3 T systems from the three major MRI vendors. The main results of this study are threefold. First, there were no significant

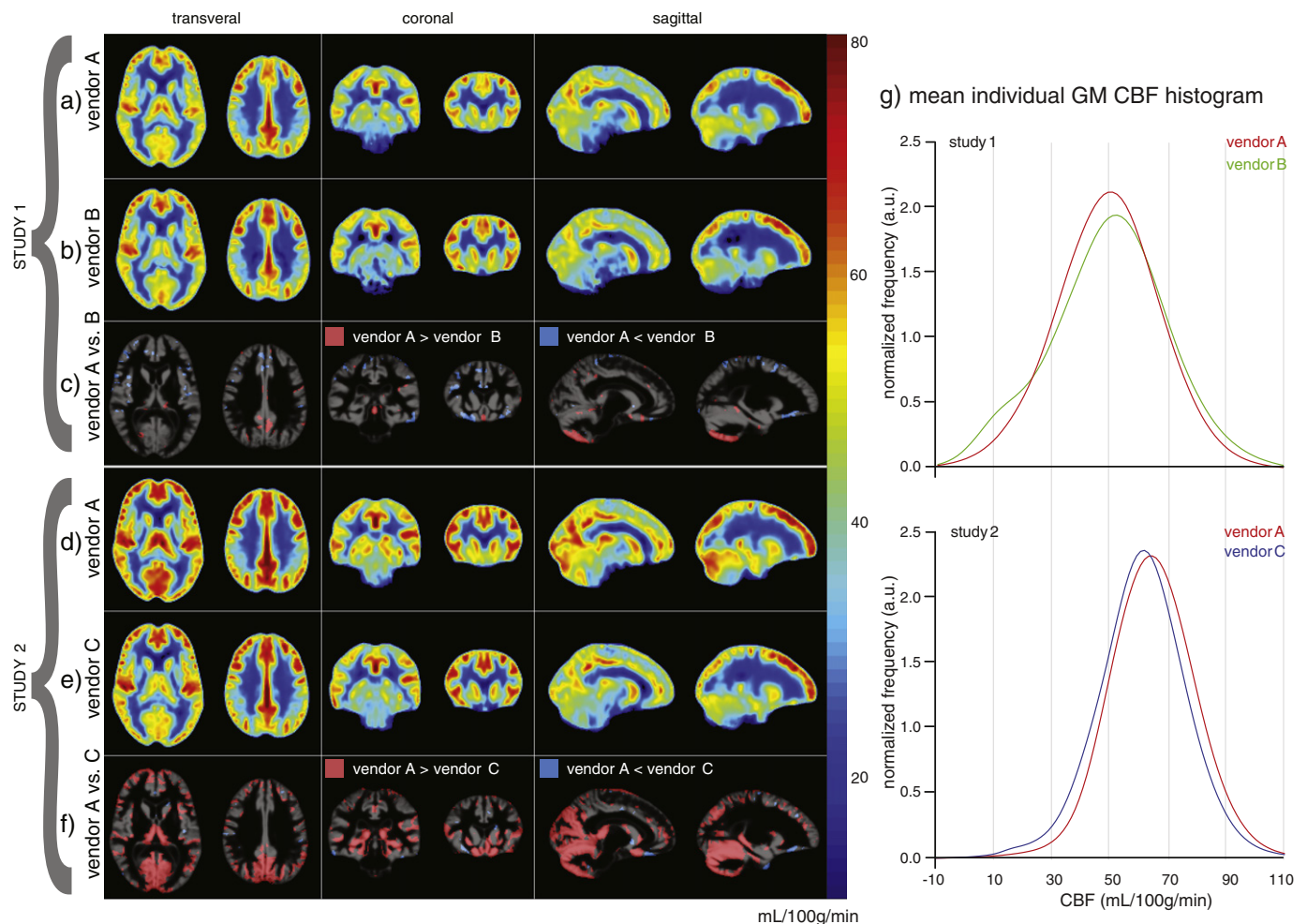


**Fig. 3.** a–b, d–e) Mean cerebral blood flow (CBF) maps; c, f) voxel-wise significant CBF differences between vendors visualized by binary parametric maps projected on the mean gray matter (GM) probability maps ( $p < 0.05$  unc.); g) GM CBF histograms.

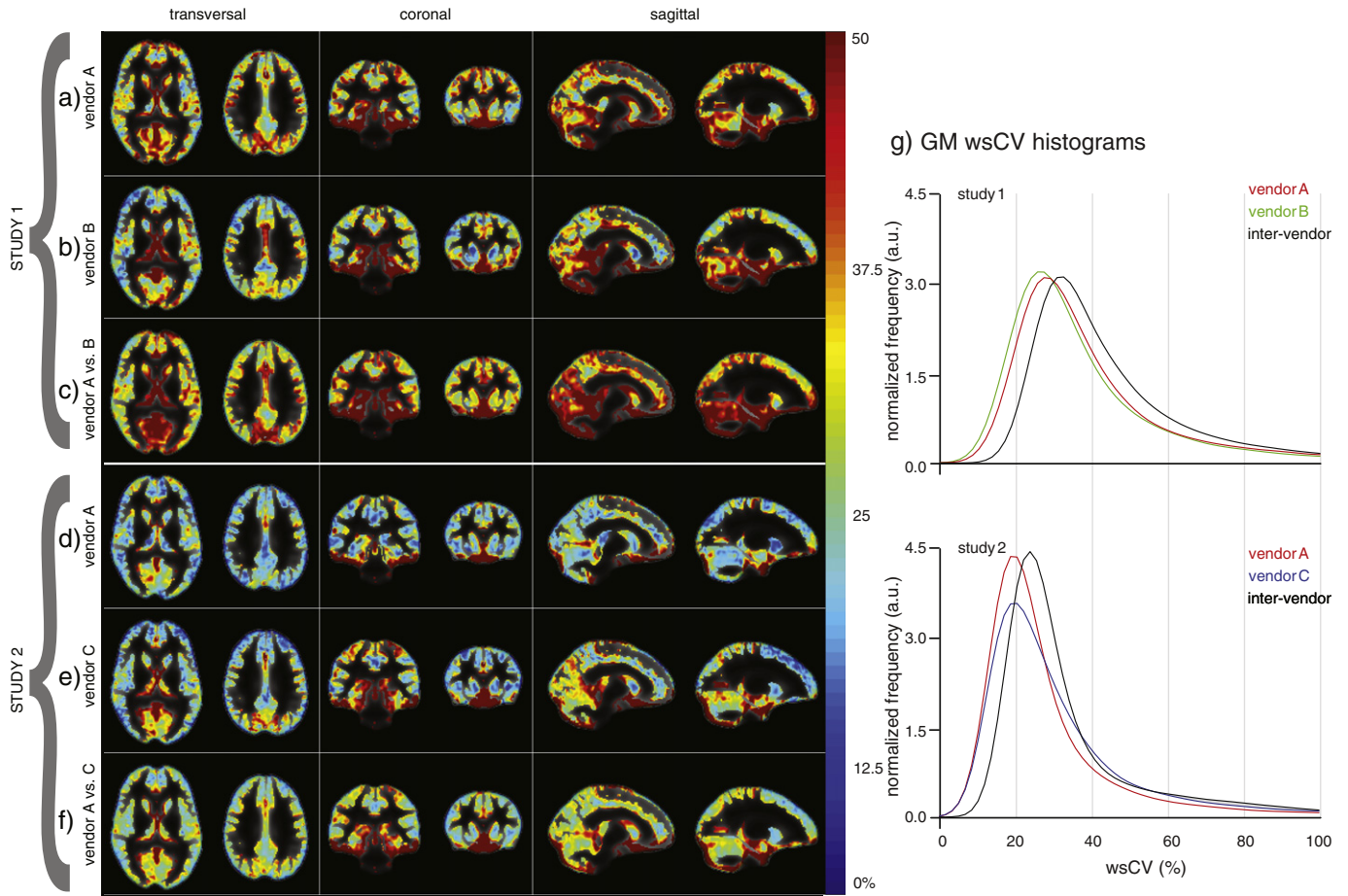


**Fig. 4.** Within-subject coefficient of variability (wsCV)-maps of study 1 (a–c) and study 2 (d–f) projected on mean gray matter (GM) probability maps; g) GM wsCV histograms.

CBF differences between vendors A and B (study 1), but there was a significant difference between vendors A and C (study 2) as well as a significant difference in CBF obtained with the sequence of study 1 versus the sequence of study 2 within the same vendor (vendor A). Second, the inter-vendor inter-session variation was larger than the intra-vendor variation, although this did not reach significance in most ROIs or voxels. Finally, for the qualitative expert ratings, the inter-vendor similarity was 9–11% lower than the intra-vendor similarity, but the inter-vendor similarity was still ‘moderate’. These results indicate that it may be possible to pool multi-vendor ASL results obtained with

near-identical sequences, but also that minor residual sequence differences can have a large effect on the reliability of ASL.

The general appearance of the CBF and wsCV-maps obtained from the current work is in agreement with what can be expected from PCASL with a 2D gradient-echo EPI readout: excellent GM–WM contrast, heterogeneously appearing GM CBF and wsCV with vascular CBF peaks and lower CBF and higher wsCV in regions sensitive to susceptibility induced artifacts such as the orbito-frontal and inferior temporal cortices (Gevers et al., 2011; Mutsaerts et al., 2014). The visual similarity of these CBF- and wsCV-maps is substantially higher than that shown in

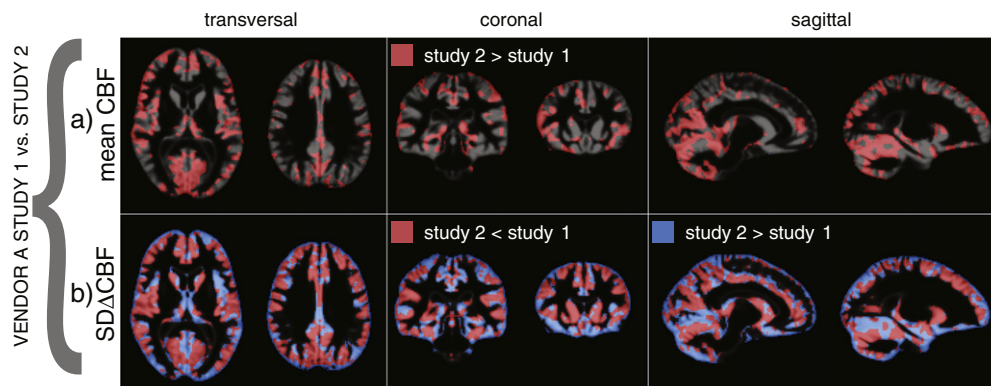


**Fig. 5.** Binary parametric maps projected on mean gray matter (GM) probability maps: a) voxel-wise significant CBF differences between studies 1 and 2 ( $p < 0.05$ ). There were no voxels for which the mean CBF of study 1 was significantly larger than the mean CBF of study 2. b) Voxel-wise significant differences in standard deviation of the paired inter-session CBF difference ( $SD\Delta CBF$ ) ( $p < 0.05$ ).

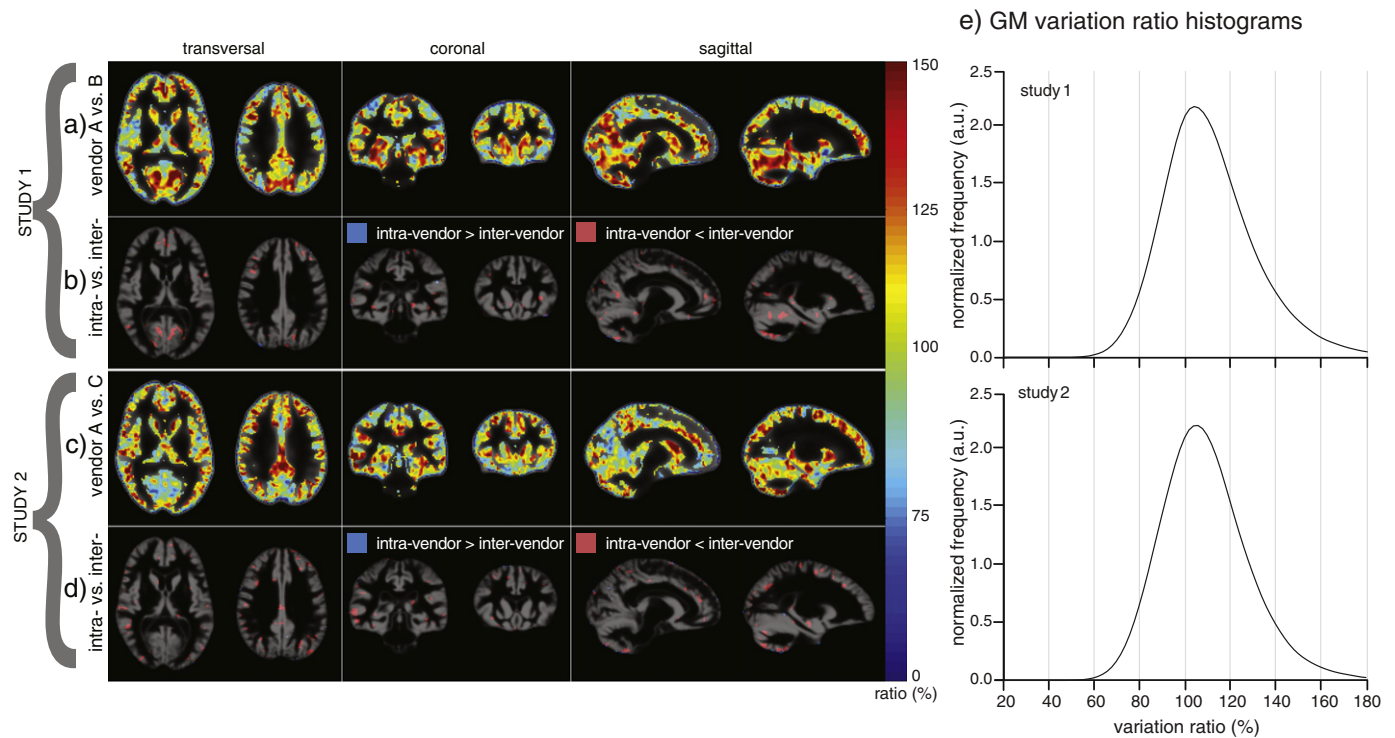


**Fig. 6.** Variation ratio. a, c) Ratio of inter- over intra-vendor standard deviation of paired inter-session differences ( $SD\Delta CBF$ ) and b, d) binary maps projected on mean gray matter (GM) probability maps, indicating for which voxels the variation ratio is significantly different from 100%. e) Gray matter variation ratio histograms.

previous multi-vendor ASL comparisons, in particular one in which a different readout (2D EPI vs. 3D spiral) was employed (Mutsaerts et al., 2014). The largest difference between vendors in that study was the difference in spatial blurring between the readouts and reconstruction as used by both vendors, which was reflected in the GM–WM CBF contrast. Whereas the GM–WM CBF ratio differed by a factor 2 between 2D and 3D readouts, this ratio was very consistent in the present results, ranging from 3.5–3.9 for all vendors (Kilroy et al., 2014; Mutsaerts et al., 2014; Vidorreta et al., 2012). This indicates that if a similar readout and reconstruction is used, ASL results are comparable between vendors, despite residual hardware differences such as differences in gradient or coil specifications. Since differences in spatial correlation can seriously affect the ability of ASL to detect regional CBF differences, these results

provide a strong argument for the importance of using the same ASL readout in multi-center studies.

To our surprise the mean and inter-session variation of CBF differed more for the same vendor across the two studies than between different vendors within the same study, both in the quantitative and qualitative analysis. These results strongly suggest that even minor sequence changes can result in a significant effect on the mean and inter-session variation of CBF. Moreover, this indicates that small differences in sequence parameters have a larger effect on the reproducibility of ASL than hardware or software differences between vendors, even when the same labeling and readout strategies are used. Future multi-center perfusion studies should therefore not only focus on keeping ASL sequence parameters as equal as possible between centers, but also within

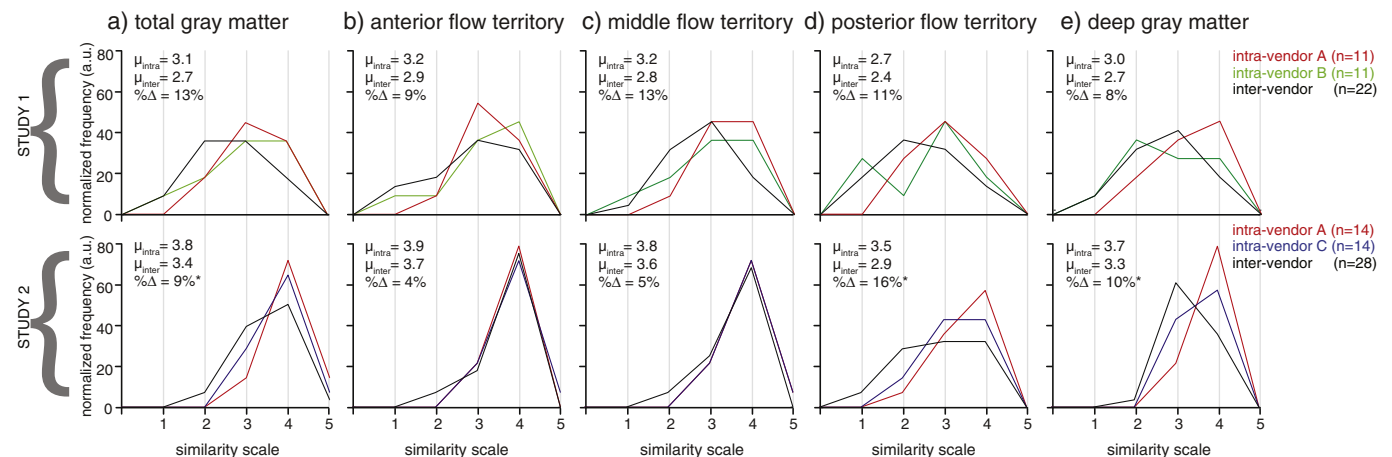


**Fig. 7.** Qualitative similarity scale histograms, 5 indicating excellent similarity and 1 indicating poor similarity. These histograms enable the comparison of visual similarity between two sessions on different vendors (black lines) with visual similarity between two sessions on the same vendor (colored lines).  $\mu$  = mean score for intra- or inter-vendor comparison,  $\% \Delta$  = percentual difference between inter-vendor and mean intra-vendor similarity (\*  $p < 0.05$ ).

a center (i.e. no software updates or upgrades resulting in small sequence changes).

The main difference between the sequences in both studies, was the inter-pulse time of the labeling RF train. The shorter interval between the labeling pulses in study 2 makes PCASL less sensitive to off-resonance degradation of the label. As no phase correction was employed, the labeling efficiency is expected to be higher in the second study (Dai et al., 2008). This can explain the higher CBF estimates found in study 2 (vendors A and C) compared to study 1 (vendors A and B). One alternative explanation for the mean CBF difference between studies could be the different slice readout times, leading to a mean effective PLD that is 100 ms longer for study 1 than for study 2. A longer PLD leads to more T1 decay, lower SNR and proportionally more spins in the tissue compartment than blood compartment – hence proportionally more faster decay with the T1 of tissue. Furthermore, the shorter effective PLD in study 2 compared to study 1 could have led to a higher proportion of vascular spins in study 2. These PLD effects lead to an arrival time dependent relative CBF underestimation for study 1 compared to study 2, which is in agreement with our results. However, the contribution of these PLD effects can be expected to be small, since the effective PLD in these studies was relatively long for young healthy subjects (Alsop et al., 2015; Wang et al., 2003). The larger T2\* decay with longer TE in study 1 reduces SNR for both the  $\Delta M$  and  $M_0$  (control) image which can partly explain its larger variation compared to study 2, both in the wsCV-maps as well as in the qualitative similarity rating. To what extent the slightly different labeling and readout parameters have contributed to the differences in mean and variation of CBF cannot be differentiated conclusively with these data.

Despite the variation differences between the studies, the inter- to intra-vendor inter-session variation ratio was very similar. The histogram showed only slightly more voxels where inter-vendor inter-session variation was larger than intra-vendor variation in study 1 (vendors A and B) compared to study 2 (vendors A and C). Again, these voxels seemed to be mainly found in the posterior region and cerebellum. This suggests that the abovementioned additional sources of variability for study 1 – such as lower labeling efficiency, larger T2\* decay and larger PLD for study 1 – have a relatively similar contribution to both the intra- and inter-vendor variability.

Whereas we observed very good agreement between the mean CBF values of vendor A and vendor B in study 1, there was a significant whole brain CBF difference between vendor A and vendor C in study 2. The largest apparent difference between the vendors in study 2 is the different receiver coils (8 versus 20 channels); contrary to study 1 where both vendors had identical 8-channel head coils. Although differences in coil sensitivity profiles are not expected to affect the CBF quantification because of the division by  $M_0$ , there may be an effect of SNR differences between coils upon the inter-session variability or CBF quantification within regions of low SNR. A post-hoc quality assurance analysis (head phantom scanned with an IEC 2D spin echo sequence, data not shown) showed that the SNR of the scanners of vendor B and C were 71% and 155% relative to vendor A (International Electrotechnical Commission (IEC), 2014; Murphy et al., 1993). However, the inter-session variation of vendor C was only lower than vendor A in the anterior orbito-frontal region and not in other areas of the brain. Perhaps, physiological variability already dominated most regions of the brain and additional SNR only helped in regions with lowest sensitivity, such as areas prone to susceptibility induced artifacts. Additional explanations for the CBF disagreement could include differences in gradient specifications, B1 field inhomogeneity or shimming of the labeling plane. The fact that the CBF disagreement between vendors A and C (study 2) was largest in the posterior flow territory can perhaps be explained by differences in labeling efficiency in the vertebral arteries. This could be attributed to differences in shimming of the labeling plane, non-identical head positions due to the different head-coil designs and to the fact that vertebral arteries are more tortuous than carotid arteries, increasing the possibility for a less perpendicular

intersection of the vertebral arteries by the labeling plane (Aslan et al., 2010). This could also explain the higher wsCV and lower qualitative similarity rates in the posterior flow territory.

It should be acknowledged that the main strength of this study is at the same time also its main weakness. The study design was optimized for an optimal similarity of pulse sequences between vendors within the same study, and not for optimal ASL SNR across all three scanners. This included the disabling of imaging enhancement features such as background suppression, parallel acceleration, partial Fourier and geometric distortion filters. These features were disabled to narrow down possible origins of inter-vendor variability, to achieve a more valid basis for comparison. Although the SNR penalty by disabling the image enhancement features were counterbalanced by longer scanning as well as scanning healthy young volunteers, the results of the current study are expected to deviate from normal clinical or research practice. These enhancement features may reduce the intra-scanner variability because of increased SNR, but may increase the inter-vendor variability because they are implementations that may vary between vendors (Vidorreta et al., 2012). It remains unknown to what extent these features can affect the multi-center reproducibility of ASL. Therefore, it is important to acknowledge that the results of this study do not in any way reflect the performance of the commercially available PCASL product sequences, since these differ significantly from the sequences that were employed in this study. This was the main reason to keep the vendor names anonymous.

Another limitation of the current study is the use of 2D sequences, whereas 3D sequences have recently been proposed as the recommended standard (Alsop et al., 2015). The practical reason for choosing a 2D readout was that the implementation and reconstruction of identical 3D sequences on all vendors was not deemed feasible at the initiation of this study. When similar implementations of 3D sequences would be available on all vendors, both the intra- and inter-vendor variability could be expected to be lower because of the relatively higher SNR of 3D readouts. Especially because of the optimal performance of background suppression for 3D readouts, which greatly improves the reproducibility of ASL (Alsop et al., 2015; Vidorreta et al., 2012). However, it remains unclear whether spatial correlation and blurring differences are smaller or larger between different 3D readouts than between 2D and 3D readouts (Vidorreta et al., 2012).

Finally, we regret that because of logistic reasons and time constraints we were unable to implement the exact same sequence on all three vendor systems. At the time of study-design, we hypothesized that the differences between the two types of implemented sequences were of little significance and that by including the two versions on vendor A a proper comparison could be performed between all three vendors. However, the results of this study showed, interestingly, that these minor sequence differences led to detectable changes in perfusion measurements. Nevertheless, we anticipate that the evaluated sequences could serve as a benchmark to compare other, more optimal, sequences between scanners from different vendors.

## Conclusion

Using near-identical ASL sequences, this multi-vendor study demonstrates the possibility to acquire comparable cerebral CBF maps on scanners from different vendors. Small differences in sequence parameters can have a larger effect on the reproducibility of ASL than hardware or software differences between vendors. These results stress the importance of using identical labeling and readout strategies when perfusion maps from multiple MRI scanners are pooled. Future efforts towards harmonization of pulse sequence approaches between vendors should pave the way for multi-center clinical perfusion studies.

## Acknowledgments

This work was founded within the COST-AID Action BM1103 (European Cooperation in Science and Technology-Arterial spin labeling Initiative in Dementia), and financially supported by a Short Term Scientific Mission (ECOST-STSM-BM1103-030114-037267) grant from this Action. This manuscript has been presented and discussed multiple times at international meetings of this Action. We thank the vendors for their support, which enabled us to implement a near-identical sequence on all three platforms. The authors are grateful to M Kleppestø and M Skurdal for help with data collection and to W.V. Potters for help with post-processing.

## Disclosure/conflict of interest

The authors declare no conflict of interest.

## References

- Alsop, D.C., Detre, J.A., Golay, X., Gunther, M., Hendrikse, J., Hernandez-Garcia, L., Lu, H., MacIntosh, B.J., Parkes, L.M., Smits, M., van Osch, M.J., Wang, D.J., Wong, E.C., Zaharchuk, G., 2015. Recommended implementation of arterial spin-labeled perfusion MRI for clinical applications: a consensus of the ISMRM perfusion study group and the European consortium for ASL in dementia. *Magn. Reson. Med.* 73, 102–116.
- Ashburner, J., 2007. A fast diffeomorphic image registration algorithm. *NeuroImage* 38, 95–113.
- Aslan, S., Xu, F., Wang, P.L., Uh, J., Yezhuvath, U.S., van, O.M., Lu, H., 2010. Estimation of labeling efficiency in pseudocontinuous arterial spin labeling. *Magn. Reson. Med.* 63, 765–771.
- Asllani, I., Borogovac, A., Wright, C., Sacco, R., Brown, T.R., Zarahn, E., 2008. An investigation of statistical power for continuous arterial spin labeling imaging at 1.5 T. *NeuroImage* 39, 1246–1256.
- Bland, J.M., Altman, D.G., 1999. Measuring agreement in method comparison studies. *Stat. Methods Med. Res.* 8, 135–160.
- Chen, Y., Wang, D.J., Detre, J.A., 2011. Test-retest reliability of arterial spin labeling with common labeling strategies. *J. Magn. Reson. Imaging* 33, 940–949.
- Dai, W., Garcia, D., de, B.C., Alsop, D.C., 2008. Continuous flow-driven inversion for arterial spin labeling using pulsed radio frequency and gradient fields. *Magn. Reson. Med.* 60, 1488–1497.
- Deibler, A.R., Pollock, J.M., Kraft, R.A., Tan, H., Burdette, J.H., Maldjian, J.A., 2008. Arterial spin-labeling in routine clinical practice, part 2: hypoperfusion patterns. *AJNR Am. J. Neuroradiol.* 29, 1235–1241.
- Detre, J.A., Rao, H., Wang, D.J., Chen, Y.F., Wang, Z., 2012. Applications of arterial spin labeled MRI in the brain. *J. Magn. Reson. Imaging* 35, 1026–1037.
- Gevers, S., van Osch, M.J., Bokkers, R.P., Kies, D.A., Teeuwisse, W.M., Majoie, C.B., Hendrikse, J., Nederveen, A.J., 2011. Intra- and multicenter reproducibility of pulsed, continuous and pseudo-continuous arterial spin labeling methods for measuring cerebral perfusion. *J. Cereb. Blood Flow Metab.* 31, 1706–1715.
- Golay, X., 2009. How to do an ASL Multicenter Neuroimaging Study. 17th ed. International Society of Magnetic Resonance in Medicine.
- Golay, X., Hendrikse, J., Lim, T.C., 2004. Perfusion imaging using arterial spin labeling. *Top. Magn. Reson. Imaging* 15, 10–27.
- Gunther, M., Oshio, K., Feinberg, D.A., 2005. Single-shot 3D imaging techniques improve arterial spin labeling perfusion measurements. *Magn. Reson. Med.* 54, 491–498.
- Heijtel, D.F., Mutsaerts, H.J., Bakker, E., Schober, P., Stevens, M.F., Petersen, E.T., van Berckel, B.N., Majoie, C.B., Booi, J., van Osch, M.J., Vanbavel, E., Boellaard, R., Lammertsma, A.A., Nederveen, A.J., 2014. Accuracy and precision of pseudo-continuous arterial spin labeling perfusion during baseline and hypercapnia: a head-to-head comparison with  $(1)(5)O$  H $(2)O$  positron emission tomography. *NeuroImage* 92, 182–192.
- Hendrikse, J., Petersen, E.T., Golay, X., 2012. Vascular disorders: insights from arterial spin labeling. *Neuroimaging Clin. N. Am.* 22, 259–2xi.
- Herscovitch, P., Raichle, M.E., 1985. What is the correct value for the brain–blood partition coefficient for water? *J. Cereb. Blood Flow Metab.* 5, 65–69.
- International Electrotechnical Commission (IEC), 2014. Magnetic Resonance Equipment for Medical Imaging – Part 1: Determination of Essential Image Quality Parameters.
- Kilroy, E., Apostolova, L., Liu, C., Yan, L., Ringman, J., Wang, D.J., 2014. Reliability of two-dimensional and three-dimensional pseudo-continuous arterial spin labeling perfusion MRI in elderly populations: comparison with  $15O$ -water positron emission tomography. *J. Magn. Reson. Imaging* 39, 931–939.
- Lu, H., Clingman, C., Golay, X., van Zijl, P.C., 2004. Determining the longitudinal relaxation time ( $T_1$ ) of blood at 3.0 Tesla. *Magn. Reson. Med.* 52, 679–682.
- Murphy, B.W., Carson, P.L., Ellis, J.H., Zhang, Y.T., Hyde, R.J., Chenevert, T.L., 1993. Signal-to-noise measures for magnetic resonance imagers. *Magn. Reson. Imaging* 11, 425–428.
- Mutsaerts, H.J., Richard, E., Heijtel, D.F., van Osch, M.J., Majoie, C.B., Nederveen, A.J., 2013. Gray matter contamination in arterial spin labeling white matter perfusion measurements in patients with dementia. *NeuroImage Clin.* 4, 139–144.
- Mutsaerts, H.J., Steketee, R.M., Heijtel, D.F., Kuijter, J.P., van Osch, M.J., Majoie, C.B., Smits, M., Nederveen, A.J., 2014. Inter-vendor reproducibility of pseudo-continuous arterial spin labeling at 3 tesla. *PLoS One* 9, e104108.
- Petersen, E.T., Mouridsen, K., Golay, X., 2010. The QUASAR reproducibility study, part II: results from a multi-center arterial spin labeling test-retest study. *NeuroImage* 49, 104–113.
- Petr, J., Ferre, J.C., Raoult, H., Bannier, E., Gauthier, J.Y., Barillot, C., 2014. Template-based approach for detecting motor task activation-related hyperperfusion in pulsed ASL data. *Hum. Brain Mapp.* 35, 1179–1189.
- Tatu, L., Moulin, T., Bogousslavsky, J., Duvernoy, H., 1998. Arterial territories of the human brain: cerebral hemispheres. *Neurology* 50, 1699–1708.
- Vidorreta, M., Wang, Z., Rodriguez, I., Pastor, M.A., Detre, J.A., Fernandez-Seara, M.A., 2012. Comparison of 2D and 3D single-shot ASL perfusion fMRI sequences. *NeuroImage* 66C, 662–671.
- Wang, J., Alsop, D.C., Song, H.K., Maldjian, J.A., Tang, K., Salvucci, A.E., Detre, J.A., 2003. Arterial transit time imaging with flow encoding arterial spin tagging (FEAST). *Magn. Reson. Med.* 50, 599–607.
- Wang, D.J., Chen, Y., Fernandez-Seara, M.A., Detre, J.A., 2011. Potentials and challenges for arterial spin labeling in pharmacological magnetic resonance imaging. *J. Pharmacol. Exp. Ther.* 337, 359–366.
- Williams, D.S., Detre, J.A., Leigh, J.S., Koretsky, A.P., 1992. Magnetic resonance imaging of perfusion using spin inversion of arterial water. *Proc. Natl. Acad. Sci. U. S. A.* 89, 212–216.
- Xu, G., Rowley, H.A., Wu, G., Alsop, D.C., Shankaranarayanan, A., Dowling, M., Christian, B.T., Oakes, T.R., Johnson, S.C., 2010. Reliability and precision of pseudo-continuous arterial spin labeling perfusion MRI on 3.0 T and comparison with  $15O$ -water PET in elderly subjects at risk for Alzheimer's disease. *NMR Biomed.* 23, 286–293.
- Ye, F.Q., Frank, J.A., Weinberger, D.R., McLaughlin, A.C., 2000. Noise reduction in 3D perfusion imaging by attenuating the static signal in arterial spin tagging (ASSIST). *Magn. Reson. Med.* 44, 92–100.